Available online at www.sciencedirect.com
ScienceDirect
Journal of Power Sources 163 (2006) 173–179
JOURNAL OF POWER SOURCES
www.elsevier.com/locate/jpowsour

Study on the LLT solid electrolyte thin film with LiPON interlayer intervening between LLT and electrodes

Jong min Lee [a,b], Soo ho Kim [a], Yongsug Tak [b], Young Soo Yoon [a,*]

[a] *Department of Advanced Technology Fusion, Konkuk University, Seoul 143-701, Republic of Korea*
[b] *Department of Chemical Engineering, Inha University, Incheon 402-751, Republic of Korea*

Received 9 August 2005; received in revised form 11 July 2006; accepted 14 July 2006
Available online 1 September 2006

Abstract

In this study, a lithium lanthanum titanate (LLT) thin film electrolyte was prepared by RF magnetron sputtering, in order to assess its potential use in solid state thin film batteries. Even though the LLT has high ionic conductivity, it cannot be used alone as a thin film electrolyte since it is chemically unstable when it comes into contact with Li metal and it has a high electronic conductivity. Lithium phosphorous oxynitride (LiPON) is stable when in contact with Li and has an extremely low electronic conductivity. We expected that the LiPON/LLT/LiPON structure would make it possible to use a LLT thin film as a thin film solid electrolyte. In order to prepare this structure, a LiPON thin film was also deposited by RF magnetron sputtering and was deposited for various times (30, 60, 90 and 120 min), in order to determine the optimum thickness ratio between LLT and LiPON. In linear sweep voltammetry measurements, the current hardly flowed in the potential range from 0 to 5.5 V in the blocking electrode and ac impedance was measured for measuring the resistance at LiPON/LLT/LiPON.

When only the LLT thin film was deposited, a current of scores of mA flowed in the operating potential range, but when an interlayer of LiPON thin film was deposited for more than 30 min on both sides of the LLT thin film, the current was less than 1 μA. Ionic conductivities of 1.11, 0.82 and 0.48×10^{-7} S cm^{-1} were observed for the deposition times of the LiPON thin film of 60, 90 and 120 min, respectively. This result suggests that the LiPON/LLT/LiPON structure might be able to be used as a thin film solid electrolyte if its ionic conductivity could be improved.

Keywords: LLT; LiPON; Ionic conductivity; Electrochemical stability

1. Introduction

The dramatic advancement in semiconductor process and circuit-design technology has accelerated the miniaturization of electronic devices. This tendency has also been applied to the field of all solid state microbatteries whose development has continued unabated, despite the extensive utilization of liquid electrolytes in the lithium batteries because the packaging size of liquid electrolytes is larger than that of solid electrolytes. Thus, the search for solid compounds with high lithium ionic conductivity which can be used as an electrolyte is very important in the development of all solid state lithium batteries [1]. Recently, even though it has been reported that lithium phosphorous oxynitride (LiPON) could be used as a solid electrolyte for thin film microbatteries, we have continued our research into the use of lithium lanthanum titanates (LLT) due to its high ionic conductivity. Inaguma et al. [1–3], Oguni et al. [4] and Kwai et al. [5] had investigated the lithium ionic conductivity of a solid solution of $La_{2/3-x}Li_{3x}TiO_3$ (LLT) compounds in the bulk state. They reported ionic conductivity was 10–100 times higher than that of LiPON at room temperature. Especially, Inaguma et al. showed that the resistance of LLT can be separated into two components, namely the resistance of the bulk part and that of grain boundary. The ionic conductivities of the bulk part and grain boundary were as high as 1×10^{-3} and 7.5×10^{-5} S cm^{-1}, respectively, with the total conductivity being 7×10^{-5} S cm^{-1}, as determined by ac impedance measurements at room temperature [1]. This result indicated that the LLT has a higher ionic conductivity than LiPON. We attempted to deposit a LLT thin film by radio frequency (RF) sputtering with various atmospheric gas ratios. However, the as-deposited LLT thin film showed several problems when it was deposited

* Corresponding author. Tel.: +82 2 2049 6042; fax: +82 2 452 5558.
E-mail address: ysyoon@konkuk.ac.kr (Y.S. Yoon).

0378-7753/$ – see front matter © 2006 Elsevier B.V. All rights reserved.
doi:10.1016/j.jpowsour.2006.07.036

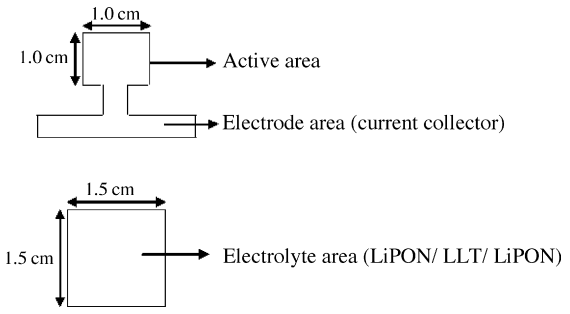

Fig. 1. Schematic plane view of top and bottom electrode patterned by metal mask (top) and LiPON-LLT-LiPON electrolyte patterned by mask (bottom).

onto the electrode directly. First, as reported by Stramare et al., when LLT was in direct contact with Li-metal, the LLT thin film was not chemically stable and underwent easy and fast Li insertion with the consequent reduction of Ti^{3+} to Ti^{4+} [6]. The other thing is potential short circuiting of the LLT thin film. In order to solve these two main problems, our research group has tried to add interlayer on both sides of the LLT. LiPON was chosen as the interlayer material, because it was thought that it would provide a good electrochemical stability in conjunction with Li electrode, as well as a relatively high short circuit voltage level as compared with the LLT. Although the LLT thin film has the above problems when it is used alone as a thin film solid electrolyte, it is still an excellent candidate for all solid state thin film microbatteries due to its high ionic conductivity.

In this work, the structural and electrochemical properties of the LiPON/LLT/LiPON multilayer structure were investigated with the use of a blocking electrode, in order to develop a new thin film solid electrolyte. In comparison with the single LLT thin film, which has various deficiencies, the LiPON/LLT/LiPON structure can be considered as a thin film solid electrolyte for all solid state microbatteries.

2. Experimental

2.1. Preparation of top and bottom electrodes (current collector)

We deposited a stainless steel (sus) thin film by a direct current (dc) sputtering with a specific pattern as shown in Fig. 1(a). The deposition time and rate measured by α-step were 25 min and 235–245 Å min^{-1}, respectively. The working pressure was 7×10^{-3} torr and dc power was 40 W (0.12–0.13 A). After making LiPON/LLT/LiPON multilayer on the bottom sus electrode, the top sus electrode was deposited on the LiPON/LLT/LiPON structure using the same conditions as those used for the bottom sus electrode.

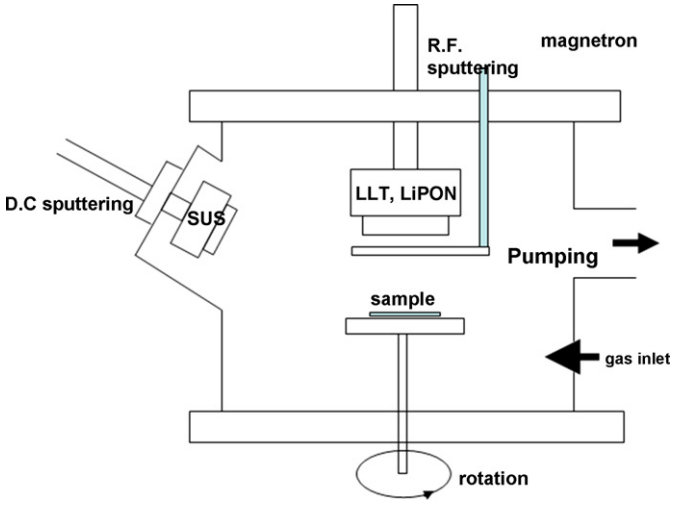

Fig. 2. Schematic diagram of the RF and dc sputtering system using sus and LLT targets.

2.2. Preparation of interlayer

After the deposition of the bottom sus electrode, the LiPON thin film was deposited on the bottom sus electrode using a 1.0 cm × 1.0 cm square type mask by RF magnetron sputtering for 30, 60, 90, 120 min as shown in Fig. 1(a). The working pressure and the RF power were 6×10^{-3} torr and 90 W, respectively. The deposition rate measured by α-step was around 415 Å/10 min.

2.3. Preparation of LLT electrolyte thin film

A 4 in.-LLT target with composition of $Li_{0.5}La_{0.5}TiO_3$ was sputtered in order to grow the LLT thin film which was deposited for 10.5 h onto the bottom LiPON layer by using the same type mask as shown in Fig. 1(b). The deposition rate measured by scanning electron microscopy (SEM) was around 75–80 Å/10 min. The working pressure was 5×10^{-3} torr and the RF powers utilized were 160, 180 and 200 W. When the LLT electrolyte layer was deposited onto the bottom sus interlayer, the sputtering power was chosen at 160 W because the LLT film had the highest relative Li content when this sputtering power was used. This was confirmed by comparing with other LLT film deposited at different RF sputtering powers. The experimental conditions are given in Table 1. Since the sputtering system for this work (as shown in Fig. 2) has both an on-axis gun and an off-axis gun, *in situ* deposition can be adopted to deposit the LLT thin film onto the bottom sus electrode. In addition, after deposition of the LLT thin film, *in situ* deposition of the top sus electrode can be carried out.

Table 1
The experimental conditions used for the deposition of the electrode, electrolyte and interlayer

	Target size (in.)	Sputter method	Sputter power	Working pressure	Chamber condition	Deposition time
sus	2	dc	40 W (0.12–0.13 A)	7 mtorr	Ar (50 sccm)	25 min
LiPON	2	RF	90 W	6 mtorr	N_2 (42 sccm)	30, 60, 90 and 120 min
LLT	4	RF	160, 180 and 200 W	5 mtorr	Ar (20 sccm)	10.5 h

2.4. Analysis of the properties of blocking electrode (sus-LiPON-LLT-LiPON-sus)

To examine the characteristics of the sus-LiPON-LLT-LiPON-sus structure, a cross-sectional image was taken by SEM analysis. The surface roughness of the LLT and the LiPON was measured by atomic force microscopy (AFM) analysis. The electrochemical stability and properties were carried out by linear sweep voltammetry (LSV) and Impedance (Zahner IM6). For the impedance measurement, copper wires were connected to the top and bottom electrodes. LSV was performed in the range of 0 to 4.5–6 V. Complex plane impedance spectra were obtained in the frequency range of 1 MHz to 10 mHz and the results are presented in the Nyquist plots. All measurements were carried out at room temperature.

3. Results and discussion

3.1. Analysis of the composition of LLT

At each sputtering power, the composition of the as-deposited LLT film was analyzed, whose metal groups and oxygen contents were measured by ICP and RBS, respectively, since ICP cannot be used to measure the oxygen content. By comparing the ICP and the RBS results, the final composition of the as-deposited film can be determined. Table 2 and Fig. 3 show the results. Based on the ICP and RBS data, the relative molar ratios according of the RF sputter were shown in Table 3. As shown in the results, the highest Li concentration was observed at 160 W. The Li composition affected the ionic conductivity of the LLT thin film. The ionic conductivity is proportional to its mobility, although at high concentrations the mobility in aqueous electrolyte is reduced (supported by the equation $\lambda_i = \mu_i(z_i \cdot F)$). However, the ion transport mechanism is different in the case of a solid electrolyte system, such as LLT, it has been reported previously that increase of Li concentration in the LLT with various Li contents induces increase of the ionic conductivity [6]. As a result, the sputtering power was chosen at 160 W. In the above equation, λ_i, μ_i, z_i and F refer to the ionic conductivity, ion mobility, the concentration of charge carrier and the Faraday constant, respectively. Even though the composition of the LLT target was $Li_{0.5}La_{0.5}TiO_3$, the reason that the concentration of Li in the as-deposited LLT film is lower than that of La and Ti is the sputtering yield for each element is different under the same glow-discharge plasma conditions: this is a typical phenomenon in the sputtering process. It has been reported that the sputtering yield of Li atom does not reach 10^{-1} (atoms/ion) until incident particle energy reaches to 10^3 eV [7]. Li and La were the A-site cations in the LLT perovskite structure (ABO_3 type). Based on the ICP and RBS data, Li and La were not sputtered in exactly the same quantities ($Li_{0.5}La_{0.5}$). In addition, the molar ratio of (Li + La)/Ti is less than 1. This result suggests that the as-deposited LLT film contains excess Ti content. Therefore, it can be speculated that the excess Ti might form the TiO_2 phase, since the oxygen affinity of Ti is extremely high during the sputtering.

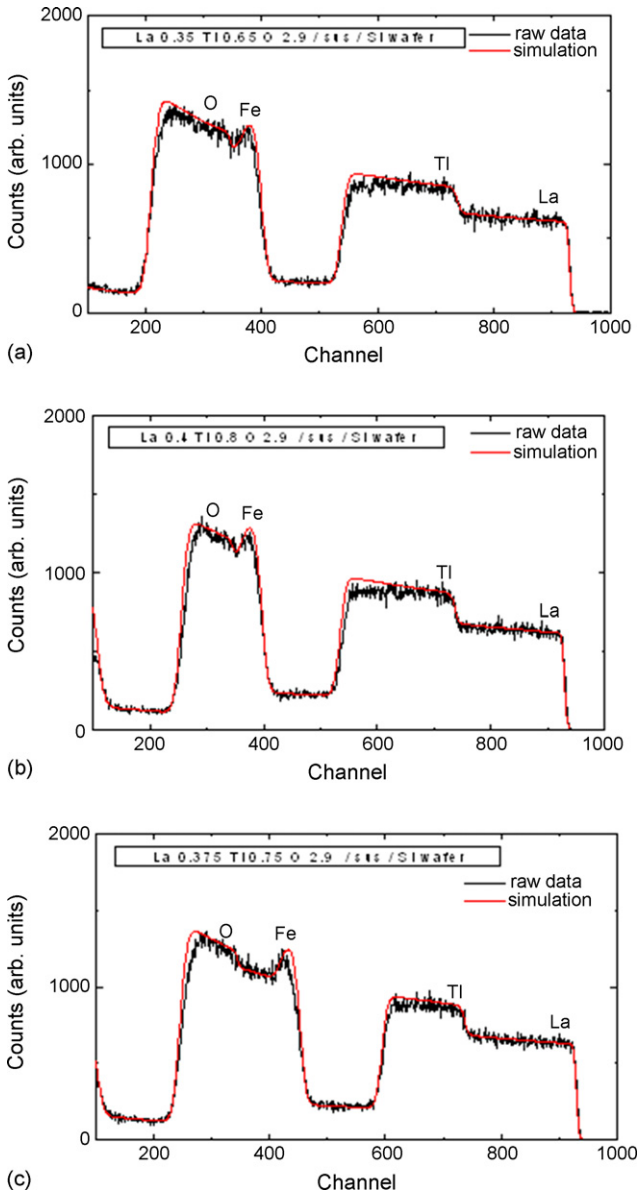

Fig. 3. RBS spectrum of LLT film deposited at 160 W (a), 180 W (b) and 200 W (c).

Table 2
ICP analysis on the surface of the deposited LLT

	Compositional analysis (mole%)		
	Li	La	Ti
Results			
160 W	0.045	0.228	0.466
180 W	0.029	0.151	0.31
200 W	0.019	0.136	0.3

Table 3
The molar ratio of each component according to RF sputter power

	Li	La	Ti	O
160 W	0.1	0.489	1	4.05
180 W	0.093	0.487	1	3.53
200 W	0.063	0.45	1	3.47

It is not expected that Li ionic conductivity will be exhibited in the TiO_2 phase, so that the presence of this phase reduces the total ionic conductivity of the as-deposited LLT film.

3.2. The physical properties of the blocking electrode

The surface roughness of the as-deposited LLT and LiPON films measured by AFM is shown in Fig. 4. The scanning area was 10 μm × 10 μm, as shown in Fig. 4. In addition, the surface scanning by AFM was conducted in 20 different areas to obtain average values. The R_{ms} surface roughness of the LLT and the LiPON films were 0.57 and 0.42 nm, respectively. Furthermore, no defects were observed on the surface. In all solid state microbatteries, the surface structural properties are very important: in this case the surface roughness of the LLT film. After the deposition of the LLT film, the top LiPON interlayer should be deposited onto this LLT film as mentioned in the experimental section. If the LLT film has defects or a high surface roughness, these can affect the growth characteristics of the top LiPON film. For example, large scale defects such as the groves and/or pores on the LLT film surface can be seen on the top LiPON film surface, which means formation of defects in an electrode film deposited onto top LiPON interlayer. That is, the defects and/or high surface roughness of the LLT film might result in the same kinds of defects being formed on the electrode as those present on the top LiPON film. These defects can act as an electronic current path or leakage source. Therefore, it is critical for the as-deposited LLT film to be defect free and have a low surface roughness surface, in order to prevent the possibility of short circuit occurrence in all solid state microbatteries. Fig. 5 shows a cross-sectional view of the blocking electrode structure (sus-LLT-sus, sus-LiPON-LLT-LiPON-sus). These images show that the thicknesses of sus, LiPON and LLT layers were 6000 Å, 2500 Å and 0.5 μm, respectively. The LiPON film thickness was able to be controlled by adjusting the sputtering time. This indicates that there was not any interface diffusion at interface between the electrode and electrolyte film, as shown in Fig. 5(b) and the SEM image of sus-LLT-sus structure allowed us to confirm its columnar structure. The grain boundary formed by the contact with these columnar grains has a high possibility for an electron transport or short circuiting. We concluded that

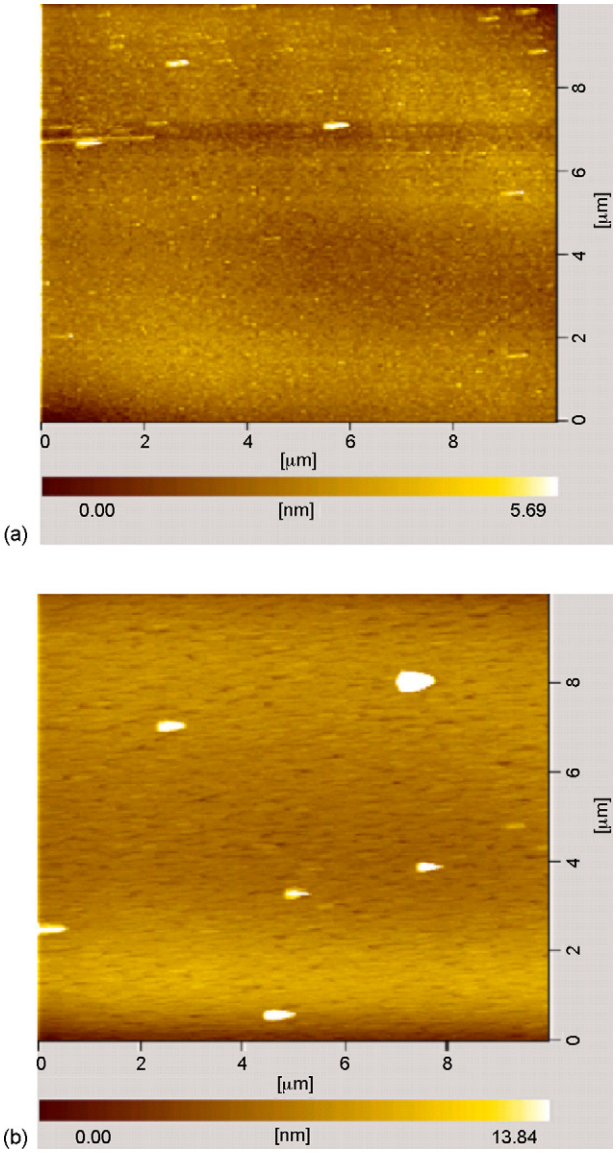

Fig. 4. The surface roughness measured by AFM after LLT (a) and LiPON (b) deposition.

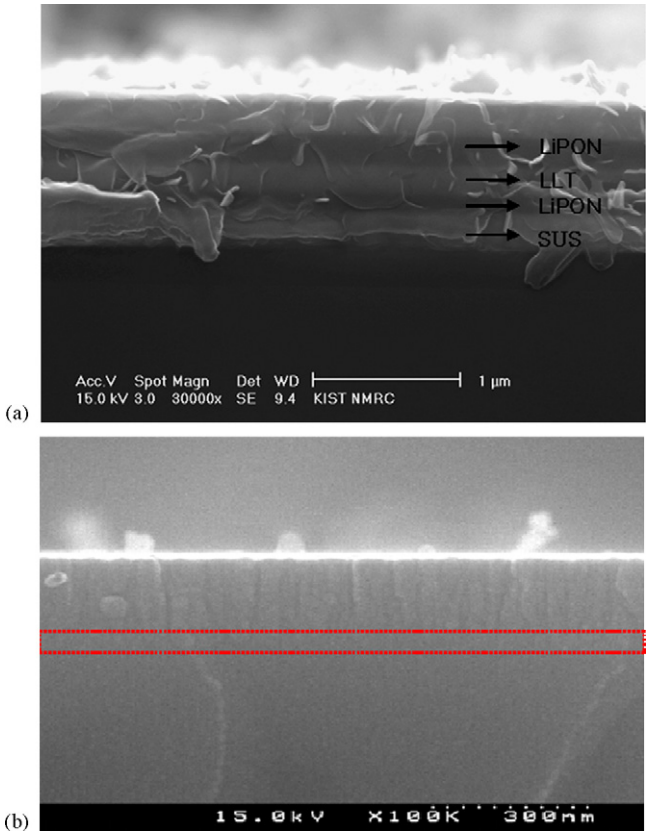

Fig. 5. Cross-sectional SEM image of the LLT film in the sus-LiPON (60 min)-LLT-LiPON-sus structure (a) and sus-LLT-sus (b). The other LiPON films deposited for different times have a similar morphology (red line in (b) indicated the interface area). (For interpretation of the references to colour in this figure legend, the reader is referred to the web version of the article.)

the columnar structure of the growth in the LLT thin film is one of the reasons for the observed short-circuit phenomenon in the sus-LLT-sus structure.

3.3. The electrochemical stability and properties of the blocking electrode

The electrochemical stability of sus-LLT-sus (single LLT) and sus-LiPON-LLT-LiPON-sus (LLT with LiPON) was determined by LSV. Fig. 6 shows its stability behavior based on a comparison with the single LLT and the LLT with LiPON (especially, LiPON deposited for 30, 60, 90 and 120 min). As shown in Fig. 6, the single LLT and the LLT with the LiPON deposited for 30 min were very unstable and happened a short-circuit in the reason shown in Fig. 5(b). However, the LLTs with LiPON with deposition times of above 30 min were very stable and subject to decomposition phenomenon at around 5.5 V. The current hardly ran between 0 and 5.5 V flowing less than 1 μA. This means that the microbattery with the LiPON-LLT-LiPON (LiPON deposited above 30 min) solid electrolyte film may show the low self-discharge during the period when it is not operating. Fig. 7(a) shows the impedance spectra measured after the fabrication of the blocking electrode. In the single LLT, the semi-circle was expressed in the Nyquist plot of blocking electrode. However, this is not indicative of ionic conductivity but electronic conductivity, which means that the single LLT could not directly apply to thin film solid electrolyte for microbatteries. In the case of the LLT with LiPON as shown in Fig. 7(b), two or three semi-circles are observed, one for each layer (LiPON, LLT and their interfaces), but we could not understand why the tail did not appear in the low frequency range. Consequently, the equivalent circuit was able to be expressed without the Warburg diffusion component. By ignoring this behavior, we were able to calculate the ionic conductivities of the LLT with LiPON with various thicknesses because total resistance of electrolyte was measured by adding the each semi-circle real part value. Inaguma et al. reported that when the impedance was measured, two semi-circles can be divided into two different contributions, namely the bulk part and the grain boundary. However, in this work, we could ignore grain boundary contribution because the as-deposited LLT film had an amorphous structure, as confirmed by XRD. As shown in Fig. 8, there was not observed any LLT crystallinity except sus and Si (silicon wafer substrate). Table 4 and Fig. 9 show the ionic conductivity according to the LiPON thickness ratio. The ionic conductivity was calculated by means of the

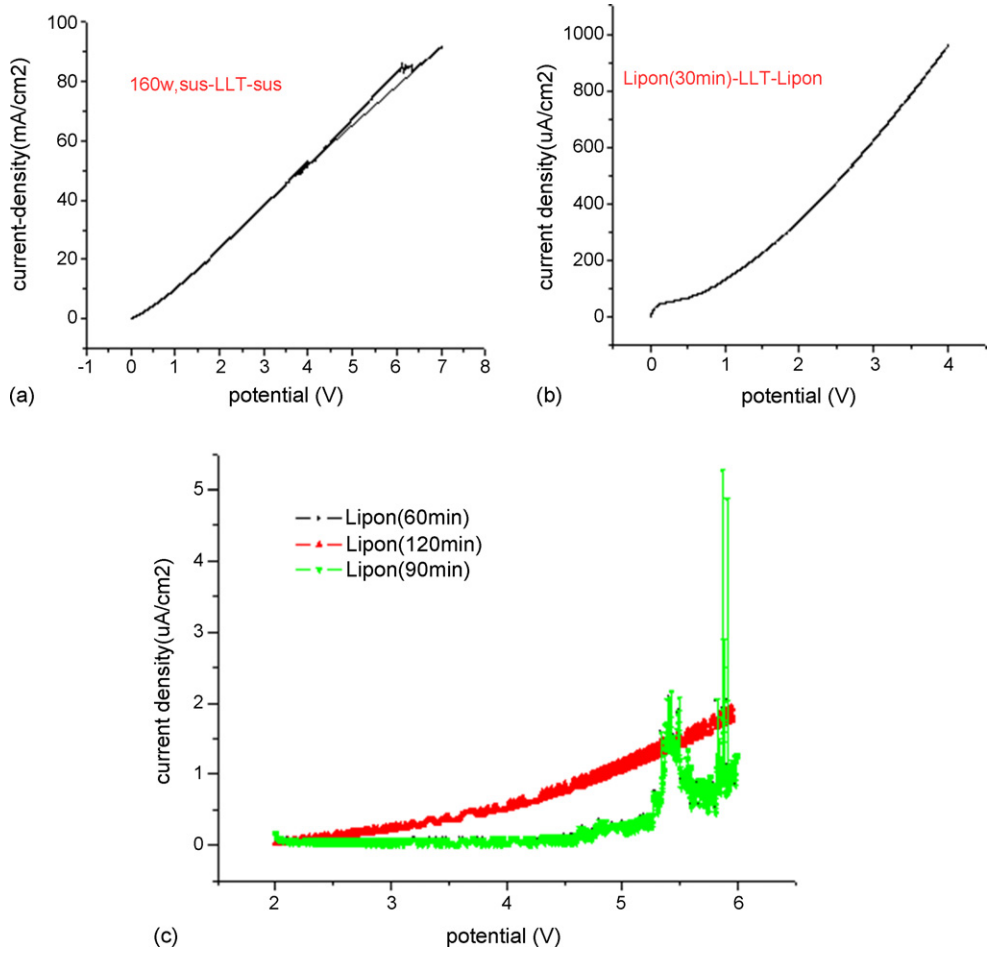

Fig. 6. The electrochemical window determined by LSV at each condition. (a) sus-LLT-sus, (b) sus-LiPON (30 min)-LLT-LiPON-sus, (c) sus-LiPON (60 min)-LLT-LiPON-sus, sus-LiPON (90 min)-LLT-LiPON-sus and sus-LiPON (120 min)-LLT-LiPON-sus.

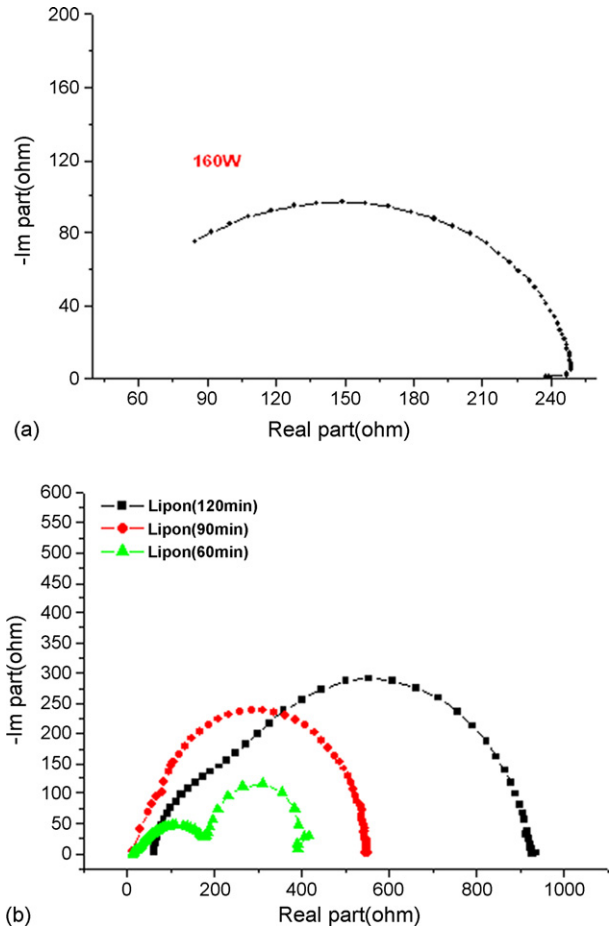

Fig. 7. Complex plane impedance spectra of blocking electrode (each condition). (a) sus-LLT-sus (LLT deposited at 160 W, this circle implies electronic conductivity) (b) sus-LiPON-LLT-LiPON-sus (LiPON deposited for more than 30 min, absence of a tail indicates that the LLT is a lithium ion conductor [6]).

following equation:

$$\sigma = \frac{d}{R \times A}\ [\mathrm{S\,cm^{-1}}]$$

d is the electrolyte thickness (LLT with LiPON), R the electrolyte resistance and A is the electrode area.

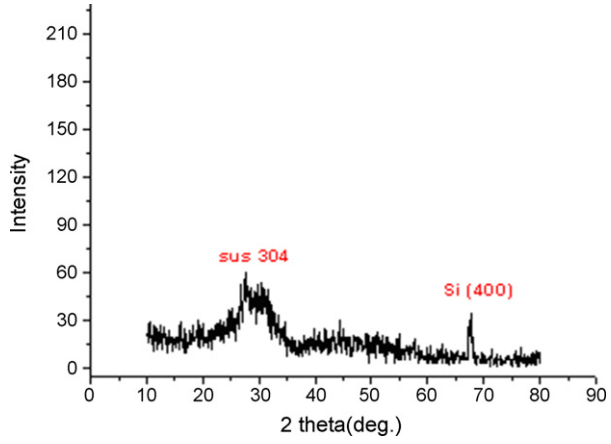

Fig. 8. XRD measurement of the sus-LLT deposited on the Si wafer without heat treatment.

Table 4
The resistance and ionic conductivity at the interlayer, LiPON, deposited for 60, 90 and 120 min

LiPON (min)	Resistance (Ω)	Thickness (LiPON + LLT)	Ionic conductivity ($\times 10^{-7}$ S cm^{-1})
60	400	1.0 μm (0.5 + 0.5)	2.50
90	545	1.1 μm (0.6 + 0.5)	2.00
120	930	1.2 μm (0.7 + 0.5)	1.29

The values for the LiPON deposited for 30 min are not given due to the occurrence of a short-circuit.

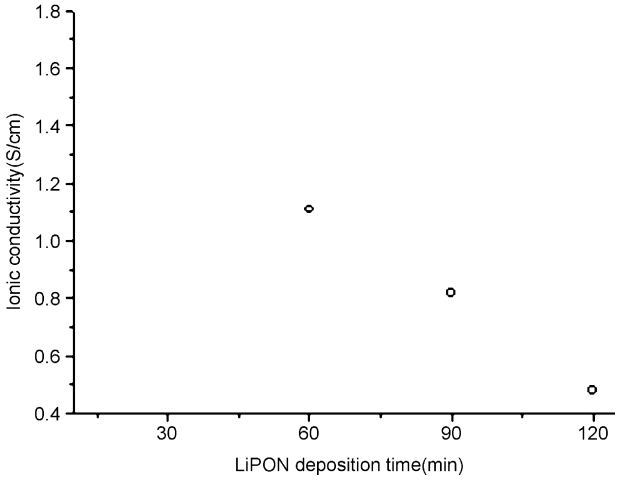

Fig. 9. The ionic conductivity diagram with various LiPON deposition times (the 30 min deposition for LiPON is not marked, due to the impossibility to obtain the measurement, ionic conductivity on the scale of 10^{-7} S cm^{-1}).

As shown in Table 3, we did not get a good ionic conductivity. Unlike in previous report (related to LLT powder, bulk state), in which the LLT thin film was deposited as a solid electrolyte by sputtering, it failed to reach 10^{-3} order S cm^{-1}. Additionally, compared with the ionic conductivity of LiPON, which reported 2–3 $\times$ 10^{-6} S cm^{-1} recently, LiPON-LLT-LiPON thin film had a poor ionic conductivity. As indicated above, this is partially attributed to the formation of TiO_2 phase during sputtering. Therefore, in order to deposit stoichiometric LLT film with a molar ratio (Li + La)/Ti of ~1, a much high concentration of Li in LLT film should be deposited by using high Li concentrated sputtering target, which prevents formation of TiO_2 phase in the LLT film.

4. Conclusion

The LLT thin film did not have a reasonable ionic conductivity and induces a short-circuit during deposition in the thin film state. The single LLT solid electrolyte thin film cannot be used for all types of solid state microbatteries, because the LLT suffers from a short-circuit problem, which can be solved by introducing an intermediate layer, such as one composed of LiPON film. An interlayer of LiPON was successfully introduced, in order to prevent the short-circuit problem when it was deposited at both sides of the LLT thin film. When the interlayer was used, the LLT

with LiPON film was very stable in the operating potential range between 0 and 5.5 V. As the LiPON with various thicknesses was deposited at both sides of the LLT film, the ionic conductivity was different at each condition. The deposition time of above 30 min, the LLT with LiPON can be utilized as an solid electrolyte, because the structure is not susceptible to the short-circuit problem. The ionic conductivities at 60, 90 and 120 min deposition of Lipon were 2.50, 2.00 and 1.29×10^{-7} S cm^{-1}, respectively.

To improve the ionic conductivity of LLT thin film, we'll try to increase the Li concentration, for example, to use LLT target with excess Li concentration.

The most important thing, in terms with LLT and LiPON thin film structure, is that LLT thin film with LiPON protective layers, helping to increase of LLT solid electrolyte stability, was tried firstly at room temperature compared to other group investigations [8,9] that were based on a powder state and a high temperature heat treatment.

Consequently, these results indicated that the LLT with LiPON structure can be applied as a thin film solid electrolyte for all-solid state microbattery.

Acknowledgement

We are grateful to the Agency for Defense Development (ADD) for their financial support and the NURICELL for their technical support.

References

[1] Y. Inaguma, L. Chen, M. Itoh, T. Nakamura, T. Uchida, H. Ikuta, M. Wakihara, Solid State Commun. 86 (1993) 689.
[2] Y. Inaguma, L. Chen, M. Itoh, T. Nakamura, Solid State Ionics 70/71 (1994) 196.
[3] Y. Inaguma, J. Yu, Y.J. Shan, M. Itoh, T. Nakamura, J. Electrochem. Soc. 142 (1995) L8.
[4] M. Oguni, Y. Inaguma, M. Itoh, T. Nakamura, Solid State Commun. 91 (1994) 627.
[5] H. Kwai, J. Kuwano, W.H. Jung, L. Chen, T. Nakamura, Solid State Ionics 70/71 (1994) 293.
[6] S. Stramare, V. Thangadurai, W. Weppner, Chem. Mater. 15 (2003) 3974.
[7] D.G. Whyte, T.E. Evans, C.P.C. Wong, W.P. West, R. Bastasz, J.P. Allain, J.N. Brooks, Fusion Eng. Des. 72 (2004) 133–147.
[8] C.H. Chen, K. Amine, Solid State Ionics 144 (2001) 51.
[9] O. Bohnke, K. Bohnke, J.L. Fourquet, Solid State Ionics 91 (1996) 21.